

UC Santa Barbara

UC Santa Barbara Previously Published Works

Title

Urban stormwater management using low-impact development control measures considering climate change

Permalink

<https://escholarship.org/uc/item/08v1k5m0>

Journal

THEORETICAL AND APPLIED CLIMATOLOGY, 154(3-4)

ISSN

0177-798X

Authors

Dougaheh, Manizheh Pourali

Ashofteh, Parisa-Sadat

Loaiciga, Hugo A

Publication Date

2023

DOI

10.1007/s00704-023-04604-z

Peer reviewed



Urban stormwater management using low-impact development control measures considering climate change

Manizheh Pourali Dougaheh¹ · Parisa-Sadat Ashofteh¹ · Hugo A. Loáiciga²

Received: 19 January 2022 / Accepted: 9 August 2023 / Published online: 26 August 2023
© The Author(s), under exclusive licence to Springer-Verlag GmbH Austria, part of Springer Nature 2023

Abstract

This work simulates rainfall using the GFDL-ESM2G large-scale model (from the Intergovernmental Panel on Climate Change-Fifth Assessment Report (IPCC-AR5)) and the change-factor method to downscale rainfall under three emission scenarios: RCP 2.6, RCP 4.5, and RCP 8.5. The Storm Water Management Model (SWMM) is applied to simulate stormwater driven by rainfall inputs in zones 1 and 3 of the northeastern municipality of Tehran under baseline (1988–2005), near-future (2030–2047), and far-future (2048–2065) conditions. The results indicate that the rainfall intensity for the design event with a 50-year return period would increase in the near future (2030–2047) and far future (2048–2065). Deployment of four types of low-impact development (LID) stormwater control measures (SCMs), i.e., vegetative swales, bio-retention cells, permeable pavement, and infiltration trenches for urban stormwater control in the study area, shows that there would be a significant change between the “with LID SCMs” condition and the “without LID SCMs” condition with respect to the flood volume at the basin outlet. The LID SCMs would reduce the flood volume in the near future by 22%, 23%, and 21% under the RCP2.6, RCP4.5, and RCP8.5, respectively, and they would reduce the flood volume in the far future by 23%, 27%, and 23% under the RCP2.6, RCP4.5, and RCP8.5 scenarios, respectively.

1 Introduction

The large impervious area of cities is conducive to the generation of large volumes of runoff laden with numerous pollutants. To compound matters, stormwater management in urban areas has become increasingly complex with the incidence of intense storms associated with climatic change. Atmosphere–Ocean General Circulation Models (AOGCMs) are applied to generate rainfall fields in urban areas with the aid of downscaling methods under greenhouse gas emission scenarios (Ashofteh et al. 2013b; IPCC 2001).

Zahmatkesh et al. (2015) investigated the performance of low-impact development (LID) stormwater control measures

(SCMs) in urban runoff management in the Brooks River Basin in New York under climate change. They used biological retention, rainfall water harvesting system, and permeable pavement stormwater control measures. Permeable pavement had the greatest effect on stormwater reduction. The latter authors found that using LID could reduce the adverse effects of climate change on future stormwater management. Gogate et al. (2017) explored sustainable alternatives for urban stormwater management in densely populated urban areas. Indicators were determined based on technical, economic, environmental, and social criteria using the analytical hierarchy process (AHP) method. The TOPSIS method was applied for ranking alternatives. The latter authors explored a framework to manage urban runoff. Aminjavaheri and Nazif (2018) studied the operation of the drainage system in one of the urban basins northeast of Tehran. They selected the most optimal locations for LID implementation using the genetic algorithm (GA). Their results indicate the efficiency of developing these systems to reduce runoff volume. Chang et al. (2018) reviewed a global LID policy for urban stormwater management. They established that the Eastern and Western worlds have different goals and attitudes towards using LID due to distinct cultural, economic, and environmental traits. Wang et al. (2018) investigated the hydrological effects and

✉ Parisa-Sadat Ashofteh
ps.ashofteh@qom.ac.ir

Manizheh Pourali Dougaheh
m.pouralidougaheh@stu.qom.ac.ir

Hugo A. Loáiciga
hloaiciga@ucsb.edu

¹ Department of Civil Engineering, University of Qom, Qom, Iran

² Department of Geography, University of California, Santa Barbara, CA 93016-4060, USA

performance of LID methods based on future modeling scenarios. Their methodology was applied to managing urban stormwater under urbanization and climate change. Eckart et al. (2018) developed a simulator-optimizer model for a sewer network considering three different return periods. Optimization was performed with Borg's multi-objective evolutionary algorithm (Borg MOEA) by considering minimizing the output runoff and minimizing the costs as goals. They found that the volume of runoff was reduced by 29%. Helmi et al. (2019) applied a LID modeling tool in Brussels for minimizing stormwater management cost. Mani et al. (2019) developed a simulator-optimizer model for LID SCM design in the sixth district of Tehran. The Multi-Objective Ant Lion Optimizer (MOALO) algorithm was applied to optimize and locate LID SCMs with the aim of reducing runoff volume in the most economical manner. Their results show that the developed simulator-optimizer model calculated suitable options for stormwater management in the region. Bahrami et al. (2019) proposed a simulation-optimization model that minimizes the costs of LID SCMs that mitigate impacts of future urban development in Tehran, Iran, relying on the stormwater management model (SWMM) coupled with the genetic algorithm (GA). Bai et al. (2019) implemented the SWMM to investigate the effects of LID SCMs on water stormwater in Suqian, China. The latter authors found that the combined use of several types of LID SCMs reduced stormwater volumes. Wang et al. (2019) investigated water storm peak discharge changes by means of bio-retention cell and porous pavement considering climate change in a basin in Guangzhou, China. Pour et al. (2020) investigated the deployment of LID SCMs to reduce the effects of urban floods caused by climate change. Saadatpour et al. (2020) developed a simulator-optimizer model for solving multi-scale and multi-parametric ponds and LID SCM placement. They applied the SWMM for stormwater simulation and the Matlab software for optimization. Liu et al. (2020) presented a hybrid runoff generation modelling framework based on spatial combination of three runoff generation schemes. The models were tested in two typical semi-humid (Dongwan) and semi-arid (Zhidan) watersheds. Hua et al. (2020) investigated the effects of LID SCMs on urban stormwater in a region of China. They found that the hazard posed by stormwater was reduced by using a combination of bio-retention cells, infiltration trenches, and rain barrels. Zhang and Ariaratnam (2020) investigated the effects of green roofs and permeable pavements on the life cycle cost (LCC) of a traditional drainage system in Arizona. Xiao et al. (2021) developed a simulator-optimizer model considering the functions of flood mitigation, reducing the area of each LID, and minimizing the cost of implementation. Oliazadeh et al. (2021) evaluated the effect of climate change on runoff management for LID SCMs in Tehran, Iran. The tropical rainfall measuring mission (TRMM) satellite precipitation data (3B42) were first

analyzed by 11 AOGCMs implemented by the IPCC. Runoff was calculated by the SWMM for different storms. Gao et al. (2021) performed the simulation and design of joint distribution of rainfall and tide level in Wuchengxiyu Region (China). Quan et al. (2022) investigated the effects of natural and social factors on atmospheric process and the hydrological cycle in Inner Mongolia (China).

Low-impact development (LID) strives to replicate or approximate the hydrological conditions that existed prior to urbanization and to retain stormwater within the area where it is generated to the extent possible (Loáiciga et al. 2015; Sadeghi et al. 2018). This study investigates the possibility of managing climate-change-affected stormwater with LID stormwater control measures.

A review of past research shows that LID SCMs have been applied to minimize peak discharge and flood volume, to improve the quality of urban stormwater, and to reduce the operating costs of flood control (Mani et al. 2019; Zahmatkesh et al. 2015). However, the application of LID SCMs to reduce the flood volume in urban areas under climate-change conditions has received less attention in the literature. This work presents a methodology for managing urban stormwater with LID SCMs. The methodology is applied to areas 1 and 3 of Tehran, Iran, under climate change conditions. The large relief that exists between Tehran and its adjacent mountainous areas causes high-elevation runoff to enter urban areas causing damaging floods. This work projects the effects of climate change on the intensity and frequency of rainfall and flood volume in the study area in the near future (2030–2047) and far future (2048–2065) under the emission scenarios RCP 2.6, RCP 4.5, and RCP 8.5 of the fifth IPCC report (IPCC-AR5). Downscaling of precipitation projections by AOGCMs is made by the change factor method.

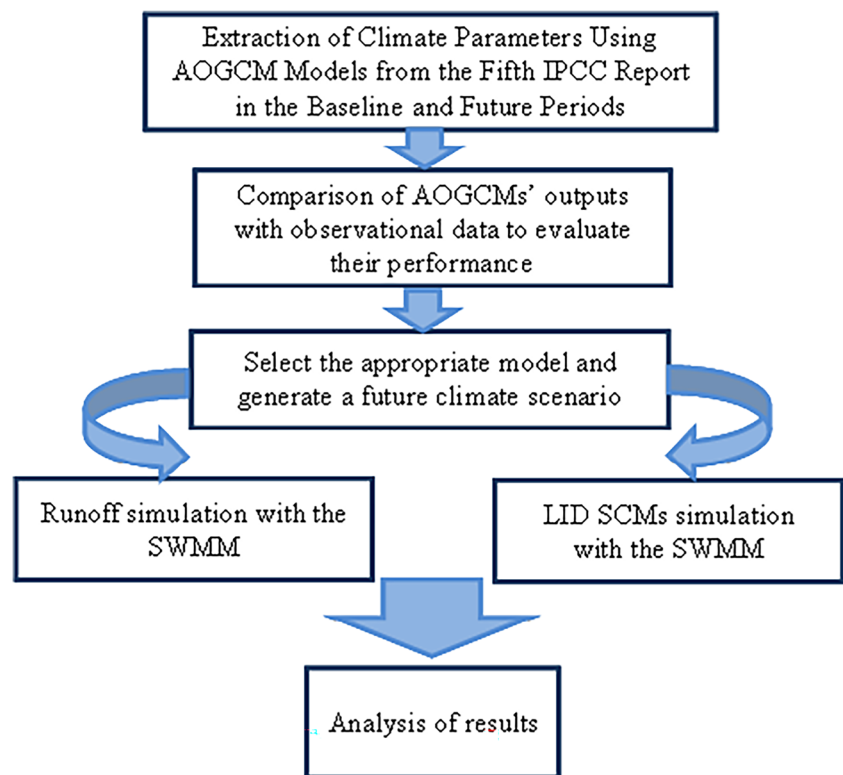
2 Methodology

The performance of climate models' climate projections reported in the fifth IPCC report is evaluated once the baseline data for the study area was gathered. The next step is to simulate the desired climatic variables in the periods under consideration. Next, the design rainfall for the study basin is determined. Stormwater is simulated with the SWMM precipitation-runoff model. Lastly, LID systems are selected according to the study area. Figure 1 displays a flowchart of this study's methodology.

2.1 Case study

The average elevation of Tehran is about 1200 m. The land surface slopes downward from north to south. To the south of Tehran are the Shahriar and Varamin plains, and to the north are the Alborz Mountains. The study area is homogeneous in terms of hydrological and physical characteristics.

Fig. 1 Flowchart of this paper's methodology



Its headwaters stem from mountainous regions north of Tehran and it extends to the Resalat highway. The study area includes the Darband, Zafaraniyeh, Elahiyeh, Qeytarieh, Amaniye, Darrous, and part of the Velenjak districts (see Fig. 2). Physical characteristics of the six sub-catchments are listed in Table 1. The average annual temperature is 16 °C and the average number of freezing days is 39 days per year. The average annual rainfall in northern Tehran is about 350 mm (Aminjavaheri and Nazif 2018).

2.2 Evaluation of climate models' performance

Projections of rainfall by 14 AOGCMs in the study area were compared to rainfall observations gathered during the 18-year-baseline period (1988–2005). For this purpose, the root mean square error (RMSE), the mean absolute error (MAE), the Nash–Sutcliffe coefficient (NSE), and the correlation coefficient (r) were applied to measure the goodness of fit of the AOGCMs' predictions (Table 2). The RMSE and the MAE evaluate the accuracy of the model based on the difference between the predicted values and the actual values, and the closer the RMSE and MAE are to zero, the better their predictions. The NSE performance criterion implies a perfect fit between the observed and the projected values when it equals one. The correlation coefficient measures the degree of linear statistical association between the observed and the projected values. A perfect positive association occurs when it equals one.

2.3 Future rainfall projections

The rainfall projections by the AOGCMs must be down-scaled to a finer spatial resolution prior to their use in the study area. The change-factor method is implemented for downscaling in this work due to its simplicity and the high speed of calculations involved (Ashofteh et al. 2013a; Zahmatkesh et al. 2015). The change-factor method downscales rainfall by first calculating the ratio of the long-term average of the rainfall simulated by AOGCMs in a period of climate change to the long-term average of the rainfall simulated by the AOGCMs in the baseline period. The monthly rainfall time series to be applied in the simulation of urban runoff with the SWMM is obtained by multiplying the ratio by the observed rainfall monthly time series (Jones and Hulme 1996).

2.4 Design rainfall of the case study

The temporal distribution and duration are key features of the design rainfall employed to generate stormwater in the study area. It is necessary to employ a design rainfall whose duration is longer than the concentration time of the study area to include runoff from all the components within the area. The Mahab Ghodss Consulting Engineers Company (2012) established that the concentration time of the entire Tehran basin to be 3 h. This implies the concentration time for the study area (which is part

Fig. 2 The study area

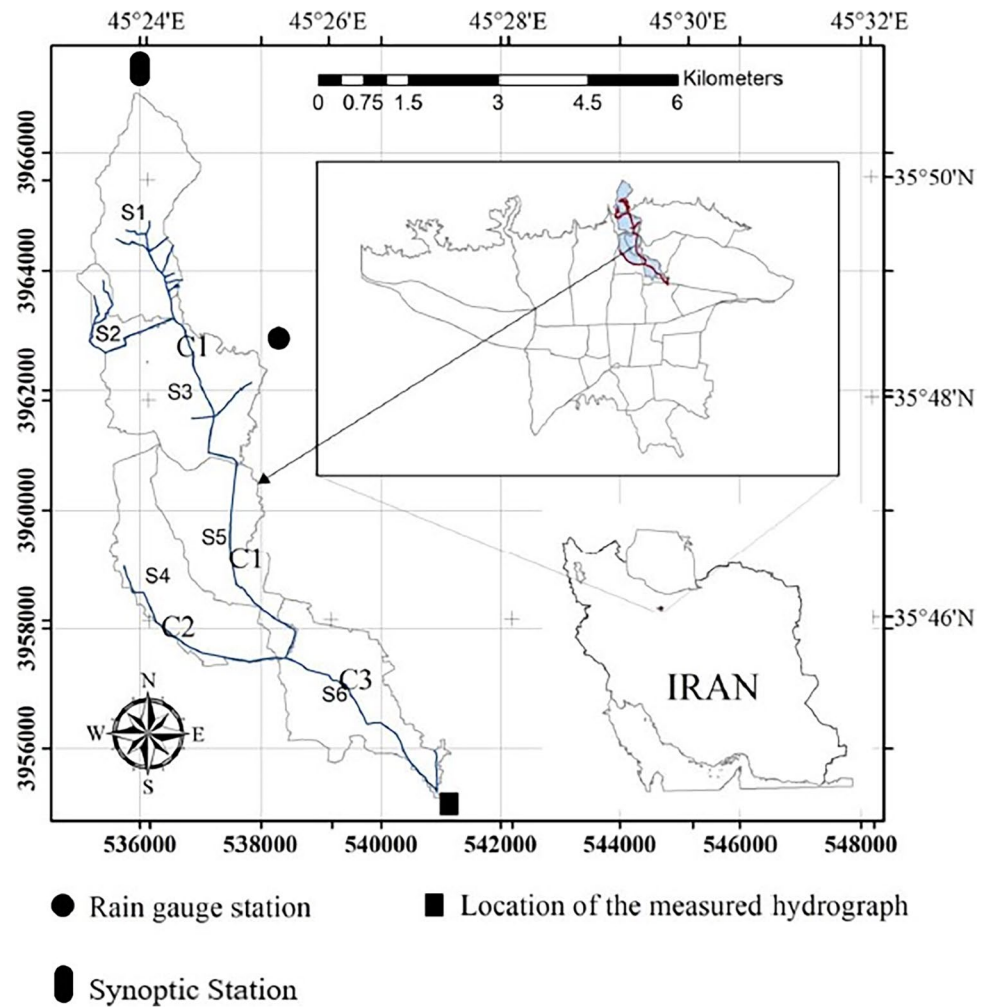


Table 1 Physical characteristics of the sub-catchments

Number of sub-catchments	Name of sub-catchments	Type of sub-catchment	Area (km ²)	Perimeter (km)	Average elevation (m)	Average slope (%)
1	S1	Mountain	4.2	14	2242	47.2
2	S2	Urban	0.8	7	1926	24.8
3	S3	Urban	4.7	15	1666	5.9
4	S4	Urban	3.9	16	1507	4.6
5	S5	Urban	3.7	15	1523	5.8
6	S6	Urban	4.1	18	1381	5.7

of the Tehran basin) is less than 3 h. This study employs a design rainfall with a return period of 50 years and duration of 6 h.

The downscaled precipitation projections for the study area are used to estimate the intensity-duration-frequency curves of rainfall in the study basin. Specifically, Eq. (1) by Ghahreman (1996) estimates rainfall events with duration from 15 min to 20 h and return periods from 2 to 100 years based on the Bell equation (Bell 1969):

$$P_T^t = [0.4524 + 0.2471 \ln(T - 0.6)] \cdot (0.3710 + 0.6184t^{0.4484}) \cdot P_{10}^{60} \tag{1}$$

$$P_{10}^{60} = 1.34(P_{24h})^{0.694} \tag{2}$$

where t is time (minutes); T return period (years); P_{10}^{60} 1-h rainfall depth with a return period of 10 years; P_T^t the calculated depth of precipitation with duration of t minutes (in mm) and return period of T (years); and P_{24h} average maximum depth of the 24-h rainfall.

Table 2 Criteria for measuring the goodness of fit of the AOGCMs' predictions

No.	Criteria
1	$r = \frac{\sum (X_s - \bar{X}_s)(X_m - \bar{X}_m)}{\sqrt{\sum (X_s - \bar{X}_s)^2 \cdot \sum (X_m - \bar{X}_m)^2}}$
2	$RMSE = \sqrt{\frac{\sum_{i=1}^N (X_s - X_m)^2}{N}}$
3	$MAE = \frac{\sum_{i=1}^N X_s - X_m }{N}$
4	$NSE = 1 - \frac{\sum_{i=1}^N (X_m - X_s)^2}{\sum_{i=1}^N (X_m - \bar{X}_m)^2}$

N stands for the number of the measured data (in here, *N* = 12 months); *X_s* simulated long-term average monthly rainfall data for each month in the baseline period (1988–2005); and *X_m* measured long-term average monthly rainfall data for each month in the corresponding period; \bar{X}_s stands for the average simulated long-term average monthly rainfall data for each month in the baseline period; and \bar{X}_m average measured long-term average monthly rainfall data for each month in the corresponding period

2.5 Rainfall-runoff simulation with the SWMM

The SWMM simulates runoff (i.e., stormwater) from rainfall. The SWMM calculates stormwater hydrographs from rain gauge, temperature, evaporation, and general meteorological data and from the characteristics of the basin and sub-basins where rainfall occurs (Zahmatkesh et al. 2015).

2.6 Selection of LID stormwater control measures (SCMs)

This work considers four LID SCMs: vegetative swales, bio-retention cells, permeable pavement, and infiltration trenches. These four SCMs were selected based on the physical and morphological characteristics of the study region. The Mahab Ghodss Consulting Engineering Company (2012) reported several studies in the study region in which the four LID SCMs cited above were applied. The LID SCMs were found to be well-suited to the physical and climatic conditions of the study region, especially when permeable pavements and infiltration trenches are used in combination and when vegetative swales and bio-retention cells are used in combination. The SCMs are input in the SWMM as layers the surface layer, the soil layer, the filter layer, and the top layer. These layers require parameters that are listed in Table 3.

3 Results and discussion

3.1 Evaluation of the AOGCMs' rainfall projections

The long-term average monthly rainfall in the baseline period calculated by 14 AOGCMs included in the IPCC fifth report was compared with the long-term average monthly rainfall observed in the same period based on the RMSE, MAE, NSE, and the *r* criteria. The results are listed in Table 4, where it is seen that the GFDL-ESM2G model featured the lowest RMSE, MAE, high *r*, and a NSE close to 1. Given this superior performance, the GFDL-ESM2G model's downscaled rainfall projections were

Table 3 Specifications for different layers in LIDs

Layer type	Parameter	LID			
		Permeable pavement	Infiltration trench	Vegetative swale	Bio-retention cell
Surface layer	Depth (mm)	80	100	500	250
	Vegetation volume fraction	0.9	0.9	0.9	0.9
	Manning roughness coefficient	0.012	0	0.24	0
	Surface slope	1	0	0.5	0
Soil layer	Porosity	-	-	-	0.35
	Thickness (mm)	-	-	-	1000
	Hydraulic conductivity of soil (mm/h)	-	-	-	250
Filter layer	Void ratio	0.2	0.7	-	0.7
	Depth (mm)	350	1200	-	150
	Hydraulic conductivity of soil (mm/h)	44	44	-	44
Top layer	Void ratio	0.15	-	-	-
	Thickness (mm)	100	-	-	-
	Permeability (mm/h)	125	-	-	-

Table 4 Goodness-of-fit criteria for evaluating AOGCMs’ rainfall projections

Model	RMSE (mm)	MAE (mm)	NSE (dimensionless)	r (%)
MRI-CGCM3	27.42	21.55	0.06	41.2
CanESM2	27.67	21.29	0.04	61.8
GFDL-ESM2M	24.24	19.30	0.27	60.7
GFDL-ESM2G	21.79	18.52	0.41	65.7
MIROC ESM-CHEM	28.26	22.67	0	49.4
CCSM4	23.51	19.32	0.31	64.9
CESM1-CAM5	23.76	20.46	0.3	68.2
NorESM1-M	22.57	18.5	0.36	73.3
MIROC-ESM	25.26	21.28	0.2	55.5
IPSL-CM5A-LR	29.66	21.65	0.01	64.8
CESM1-WACCM	30.98	25.42	0.02	63.5
MIROC5	25.69	19.81	0.18	70.4
CESM1-FASTCHEM	24.37	20.12	0.26	54.7
BNU-ESM	25.80	19.21	0.17	87.7

Values in bold indicate the acceptable performance for simulating rainfall projections

chosen for simulating stormwater under climate change in the study area.

3.2 Rainfall projections

The GFDL-ESM2G model’s downscaled rainfall projections were used to calculate the design rainfall under

the RCP 2.6, RCP 4.5, and RCP 8.5 emission pathways. The results of changes in the long-term monthly average rainfall in the near-future and far-future periods projected by the GFDL-ESM2G model are presented in Table 5 and Fig. 3. Table 5 and Fig. 3 indicate that all scenarios (except for the RCP 2.6 scenario in the near future) project a decline in the average annual long-term rainfall in the future years. The decline in rainfall would be more accentuated in the near future. The largest decline in the average long-term annual rainfall in the near future corresponds to the RCP 8.5 scenario and in the far future to the RCP 2.6 scenario. The smallest decline in the long-term annual average rainfall in the near future compared to the baseline period corresponds to the RCP 4.5 scenario, and in the far future, it corresponds to the RCP 8.5. Figure 3 shows that the long-term average monthly rainfall under climate change compared to the baseline period would increase mainly in the autumn (November and December) and spring (May and June). Also, the long-term average monthly rainfall under climate change compared to the baseline would decrease mainly in winter and summer (August and September).

3.3 Stormwater simulation

The SWMM runoff management model is a dynamic rainfall-runoff simulation model that is used for quantitative and qualitative simulation of a rainfall event or for long-term simulation of runoff in developed urban areas. This work

Table 5 Changes in the long-term average monthly rainfall for the far and near future and the baseline period

Month	Average of long-term rainfall (mm)						
	Baseline	Future (2030–2047)			Future (2048–2065)		
		RCP 2.6	RCP 4.5	RCP 8.5	RCP 2.6	RCP 4.5	RCP 8.5
Jan	63.05	44.08	50.22	41.01	43.52	46.71	52.73
Feb	65.66	45.34	36.23	39.54	41.41	43.77	23.81
Mar	83.34	56.38	69.64	63.80	59.30	62.27	62.45
Apr	49.14	44.37	45.50	52.54	31.32	32.74	41.99
May	25.79	58.48	51.58	47.02	34.17	34.23	48.50
Jun	4.04	12.24	17.23	8.96	12.81	11.48	10.04
Jul	4.25	9.03	5.49	7.09	9.57	7.91	5.31
Aug	3.22	1.05	0.96	1.55	0.80	0.69	1.05
Sep	3.41	1.06	1.48	1.09	1.02	1.01	0.75
Oct	16.53	8.44	5.76	7.04	7.57	6.52	6.29
Nov	41.35	76.94	54.13	59.90	61.15	64.30	54.63
Dec	66.26	83.92	78.62	86.57	76.41	71.14	78.62
Long-term annual average	35.5	36.78	34.74	34.68	31.59	31.90	32.18
The difference between the long-term monthly average of future and baseline rainfall	-	1.28	- 0.77	- 0.83	- 3.92	- 3.61	3.32
Percentage changes (increase or decrease) of the long-term average monthly future rainfall compared to the baseline)	-	3.59	- 2.15	- 2.33	- 11.03	- 10.16	- 9.36

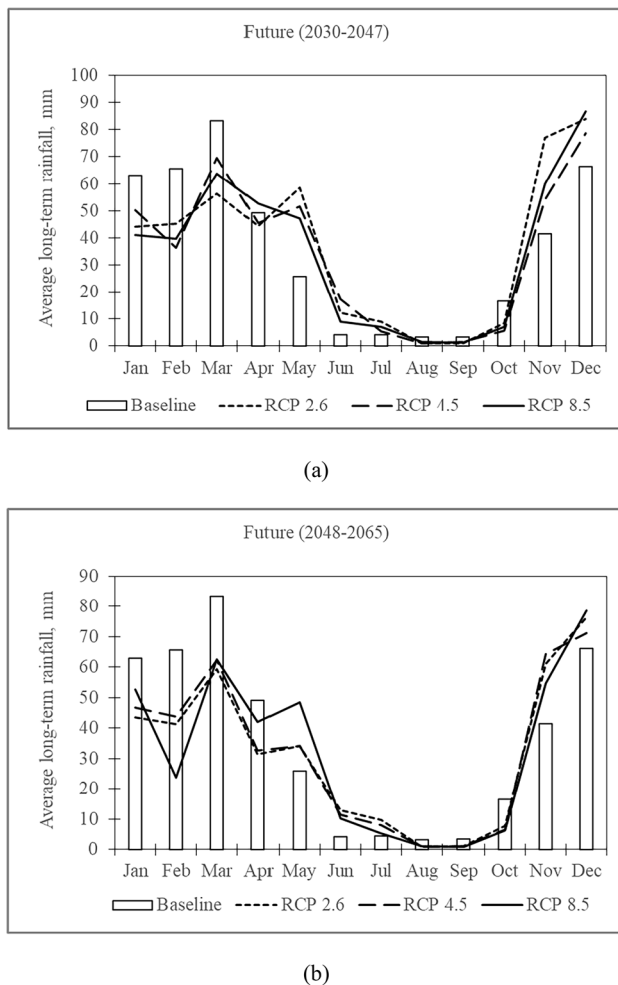


Fig. 3 Comparison of long-term average monthly rainfall for **a** near future (2030–2047) and **b** far future (2048–2065)

implemented the SWMM (Aminjavaheri and Nazif 2018; Mahab Ghodss 2012). Infiltration was calculated with the Soil Conservation Service curve number. The kinematic wave method was used for stormwater routing.

3.4 The temporal rainfall pattern in the future and baseline periods

The alternating block method (see, e.g., Chow et al. 1988) was used to develop the temporal rainfall pattern of the design rainfall in the study region. The intensity of rainfall in intervals of 15 min to 6 h (the duration of the design rainfall) was determined using Eq. (1), and the depth of rainfall in every time step was calculated with the alternating block method. Figure 4 displays the hyetograph and the cumulative depth of design rainfall corresponding to the near-future and far-future periods under the RCP8.5 and RCP 2.6 scenarios. The rainfall patterns are similar but not identical. Figure 4 shows that rainfall intensity would increase in all scenarios

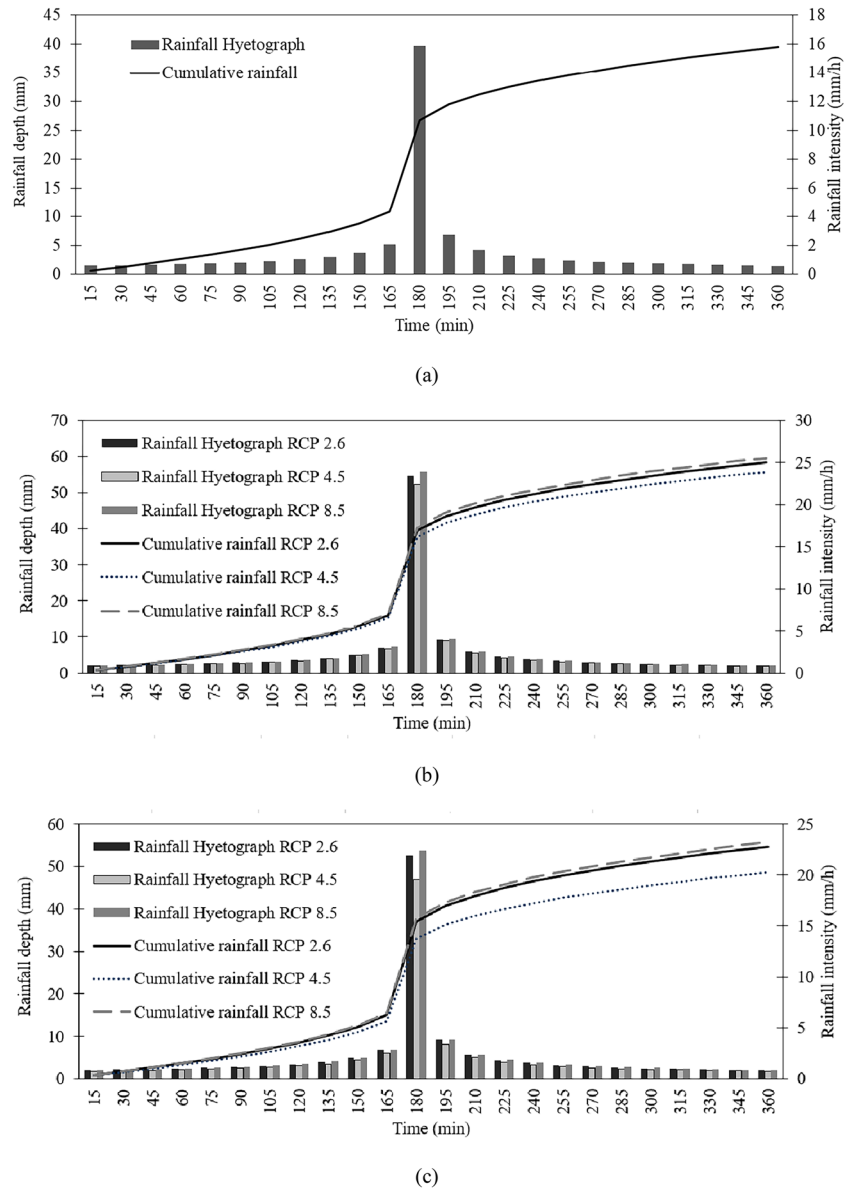
(except RCP 4.5 in the far future) in the future years compared to the baseline period. The results and calculations established that the smallest reduction in rainfall intensity in the near and far future compared to the baseline period is projected to occur in the RCP 4.5 scenario. The rainfall calculation results establish that the increase in rainfall intensity in the near future would be higher than in the far future. The largest increase in the near and far future relative to the baseline period corresponds to the RCP 8.5 scenario. The smallest reduction of rainfall in the near and far future compared to the baseline period corresponds to the RCP 4.5 scenario. Equations (1) and (2) establish that the maximum average depth of 24-h rainfall is required to calculate the depth of rainfall. This depth occurs in the rainy seasons, and the long-term average monthly rainfall would increase in the rainy seasons under climate change compared to the baseline period. The increase in rainfall intensity is therefore consistent with the rise in long-term average rainfall under climate change.

3.5 Stormwater simulations

The performance of stormwater drainage system with and without LID SCMs was evaluated. Flood nodes (large dots) caused by the design rainfall without LID in the near and far future under different RCPs are depicted in Fig. 5, and those with LID are presented in Fig. 6. Stormwater was simulated with and without the LID SCMs in the study area. The results are shown in Table 6, where it is seen that without the LID SCMs under climate change with respect to the emissions scenarios, the number of flood nodes in the study area would increase compared to the baseline period. The flood volume in node 7, which is the most critical node in the study area, would increase. The flood volume would increase the most under all emission scenarios in the near future without the use of LID SCMs because the increase in rainfall intensity in the near future would be greater than in the baseline period and in the far future. More flood nodes would occur in the near future under the RCP 8.5 scenario, and the flood volume at critical node 7 would exhibit the largest value compared to the other two other emission scenarios. The number of flood nodes, including the flood volume at 7 nodes, would decline in the far future. The number of flood nodes would be larger under the RCP 8.5 scenario than under the two other scenarios due to the near-future rainfall intensity and flood volume at node 7.

Deployment of LID SCMs in the baseline period would produce a 100% reduction in flood volume. Deployment of LID SCMs in the near future would reduce the flood volume by 61, 69, and 41% under the RCP 2.6, RCP 4.5, and RCP 8.5 scenarios, respectively. The largest rate of change occurs under the RCP 4.5 scenario, which is due to the lower

Fig. 4 Hyetograph and depth of the 6-h, 50-year design rainfall in the study basin in **a** baseline condition, **b** near future (2030–2047), and **c** far future (2048–2065)



rainfall intensity in this scenario. Also, in the far future and with the deployment of LID SCMs, the rate of flood reduction would reach 71%, 80%, and 69% under the RCP2.6, RCP4.5, and RCP8.5, respectively. These results indicate that the rate of reduction of flood volume in the far future would be larger than in the near future with and without LID SCMs.

The results in Table 6 indicate that in the baseline period, floods would occur at one node and the volume of flood in the basin without LID SCMs would be 9.904×10^6 l, and with LID SCMs, there would not be flood nodes in the basin, showing that the deployment of the LID SCMs would prevent floods in the study area.

The number of flood nodes in the near future (2030–2047) under the RCP2.6 scenario would change from one node in

the baseline period to six nodes. It is seen in Table 6 that by using LID SCMs, four flood nodes would vanish and the rate of flood reduction at different nodes under this scenario would vary from 52 to 100%, and node 7, which would have the largest flood volume without LID SCMs, would experience a reduction of 50% of the flood volume with the deployment of LID SCMs. The number of flood nodes would be changed from one node in the baseline period to three nodes under the RCP4.5 scenario. The deployment of LID SCMs would eliminate one flood node and the reduction of the flood volume would be in the range of 64 to 100%, and at node 7, which is the critical node of the drainage system in the study area, the flood volume would be reduced by 64%. The number of flood nodes would increase to seven nodes under the RCP8.5 scenario. The results of Table 6

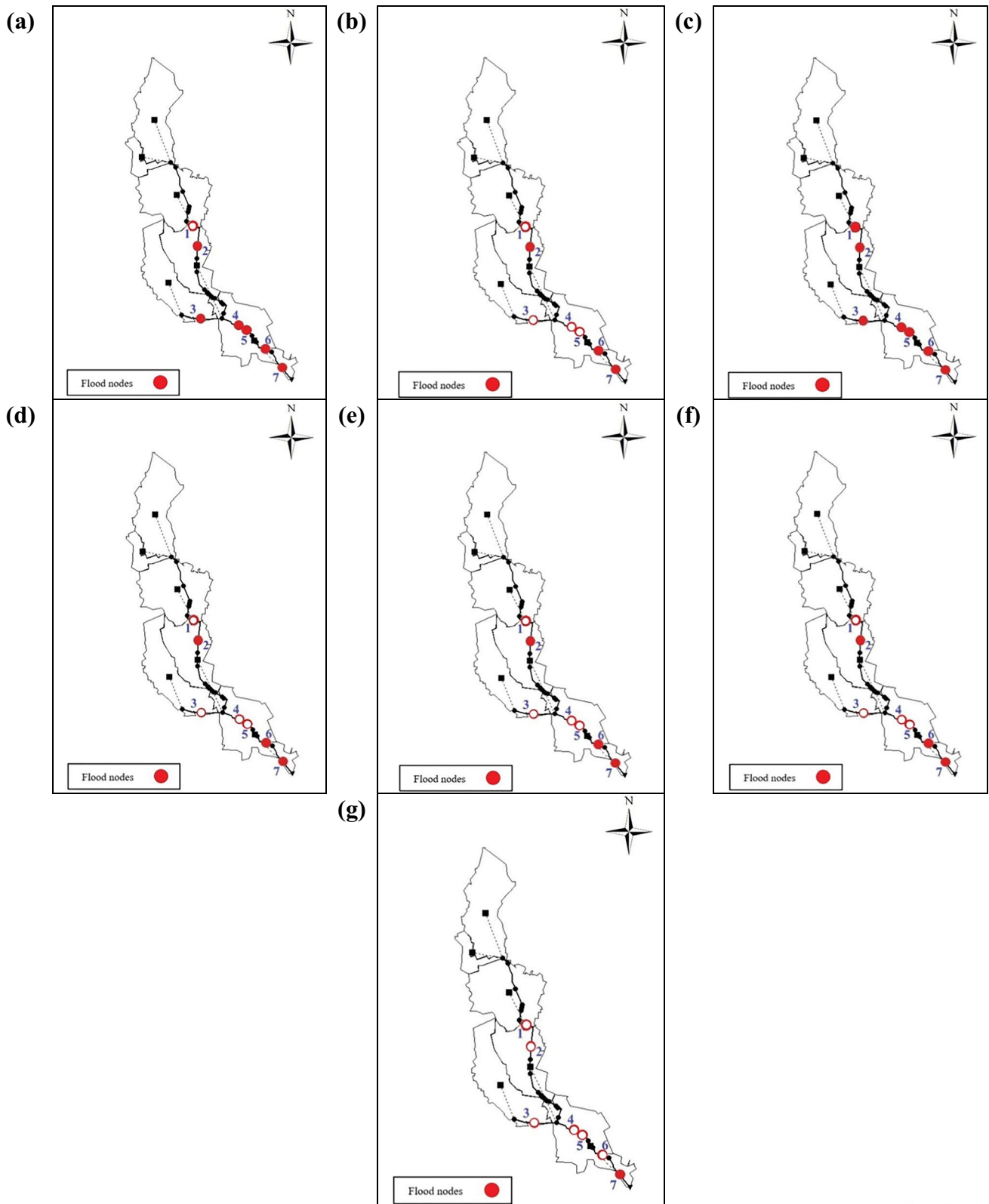


Fig. 5 Flood nodes (large dots) caused by the design rainfall without LID in the near future (2030–2048) for the **a–c** RCP2.6, RCP4.5, and RCP8.5; in the far future (2048–2065) for the **d–f** RCP2.6, RCP4.5, and RCP8.5; and **g** in the baseline

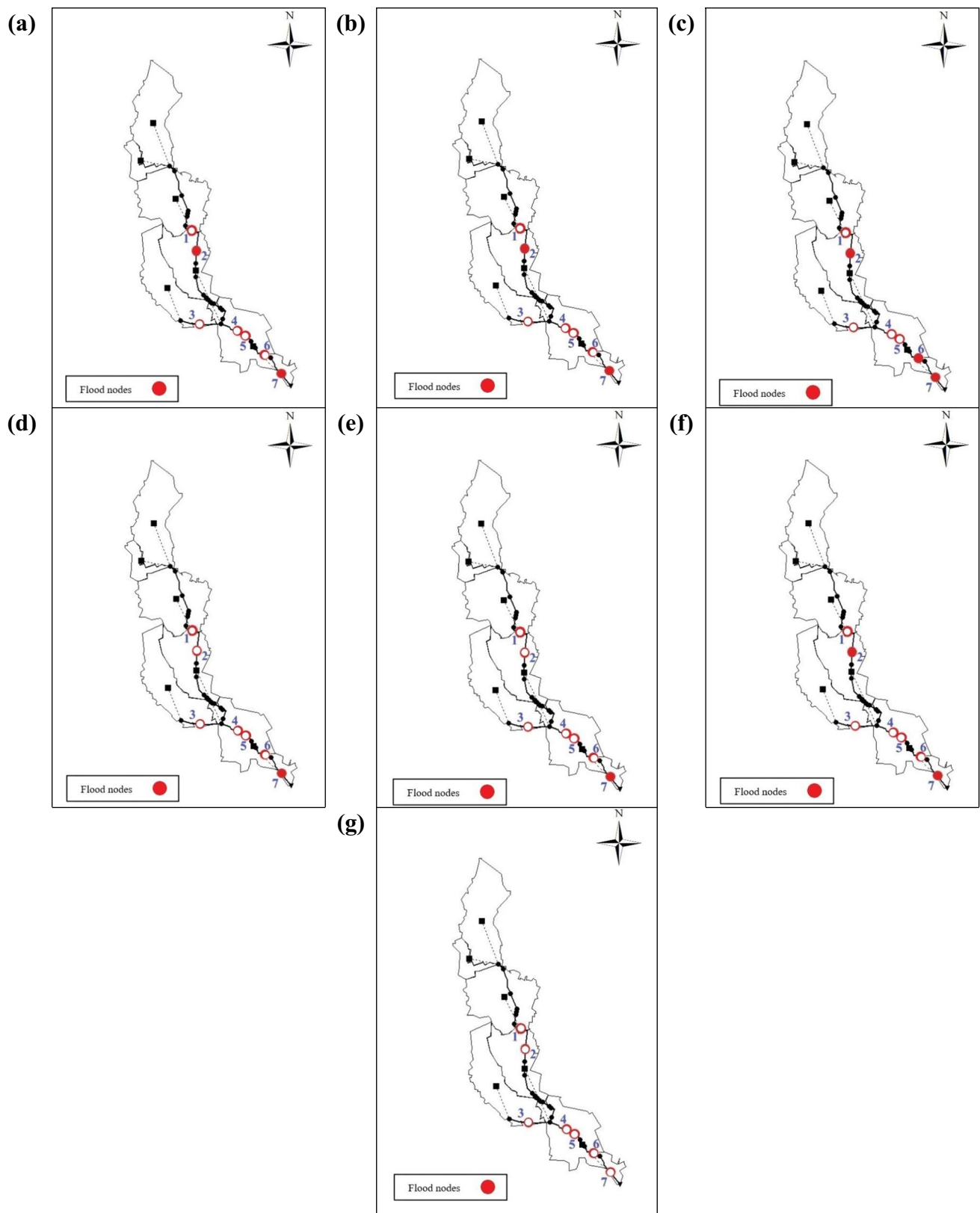


Fig. 6 Flood nodes (large dots) caused by the design rainfall with LID in the near future (2030–2048) for the **a–c** RCP2.6, RCP4.5, and RCP8.5; in the far future (2048–2065) for the **d–f** RCP2.6, RCP4.5, and RCP8.5; and **g** in the baseline

Table 6 Results at the flood nodes corresponding to the future and baseline periods

Period	Emission scenario	Flood node	Flood volume without LID (liters)	Flood volume with LID (liters)	Flood volume decreased (liters)	Percentage reduction in flood volume (%)
Baseline (1988–2005)	-	7	$10^6 \times 9.904$	0	$10^6 \times 9.904$	100
Near future (2030–2047)	RCP 2.6	7	$10^6 \times 51.202$	$10^6 \times 24.186$	$10^6 \times 27.016$	52.76
		6	$10^6 \times 7.804$	0	$10^6 \times 7.804$	100
		5	$10^6 \times 0.556$	0	$10^6 \times 0.556$	100
		4	$10^6 \times 0.002$	0	$10^6 \times 0.002$	100
		3	$10^6 \times 0.306$	0	$10^6 \times 0.306$	100
	RCP 4.5	2	$10^6 \times 4.336$	$10^6 \times 0.628$	$10^6 \times 3.708$	85.51
		7	$10^6 \times 46.788$	$10^6 \times 16.798$	$10^6 \times 29.99$	64.09
		6	$10^6 \times 5.318$	0	$10^6 \times 5.318$	100
		2	47	$10^6 \times 0.098$	$10^6 \times 2.884$	96.71
		7	$10^6 \times 53.524$	$10^6 \times 21.179$	$10^6 \times 26.345$	49.22
	RCP 8.5	6	$10^6 \times 9.012$	$10^6 \times 0.053$	$10^6 \times 8.959$	99.41
		5	$10^6 \times 0.992$	0	$10^6 \times 0.992$	100
		4	$10^6 \times 0.003$	0	$10^6 \times 0.003$	100
		3	$10^6 \times 0.602$	0	$10^6 \times 0.602$	100
2		$10^6 \times 5.026$	$10^6 \times 0.97$	$10^6 \times 4.056$	80.70	
Far future (2048–2065)	RCP 2.6	1	$10^6 \times 0.062$	0	$10^6 \times 0.062$	100
		7	$10^6 \times 45.082$	$10^6 \times 14.576$	$10^6 \times 30.506$	67.66
		6	$10^6 \times 4.298$	0	$10^6 \times 4.298$	100
	RCP 4.5	2	$10^6 \times 2.465$	0	$10^6 \times 2.465$	100
		7	$10^6 \times 30.514$	$10^6 \times 5.938$	$10^6 \times 24.576$	80.54
		6	$10^6 \times 0.357$	0	$10^6 \times 0.357$	100
	RCP 8.5	2	$10^6 \times 0.361$	0	$10^6 \times 0.361$	100
		7	$10^6 \times 46.788$	$10^6 \times 16.798$	$10^6 \times 29.99$	64.09
		6	$10^6 \times 5.318$	0	$10^6 \times 5.318$	100
		2	$10^6 \times 2.982$	$10^6 \times 0.098$	$10^6 \times 2.884$	96.71

indicate that by using LID SCMs, four flood nodes would be eliminated and the reduction of the flood volume varies from 49 to 100%, and the flood volume at node 7 would be reduced by 50%.

The number of flood nodes would involve three nodes (in comparison to one node in the baseline condition) in the far future (2048–2065) under the RCP2.6 scenario. The deployment of the LID SCMs would result in the elimination of two flood nodes and in the reduction of flood volume in the range of 67 to 100%. Node 7 would have a 67% reduction in the flood volume with the installation of the LID SCMs. The number of flood nodes would rise from one node in the baseline condition to three nodes under the RCP4.5 scenario. The results in Table 6 indicate that deployment of the LID SCMs would eliminate two flood nodes and the flood volume at node 7 would be reduced by 80%. The number of flood nodes would rise from one node in the baseline condition to three nodes under the RCP8.5 scenario. The LID SCMs would eliminate a flood node and the flood volume at node 7 (the critical node) would be reduced by about 64%.

Some nodes, such as node 7, which is located at the outlet of the basin, receive a large volume of stormwater from other nodes. Yet, the reduction of flood volume by the deployment of LID systems at this node is noticeable. These findings are highlighted by graphing the results of Table 6 in Fig. 7.

4 Concluding remarks

Evaluation of fourteen models implemented in the fifth IPCC report revealed that the FDL-ESM2G model produced the best rainfall projections of rainfall in the near future (2030–2047) and the far future (2048–2065) under the emission scenarios of RCP 2.6, RCP 4.5, and RCP 8.5.

The results show that all scenarios (except for RCP 2.6 in the near future) would experience a reduction in the average long-term annual rainfall in the future years compared to the baseline period. The reduction in rainfall would be greater in the far future than in the near future.

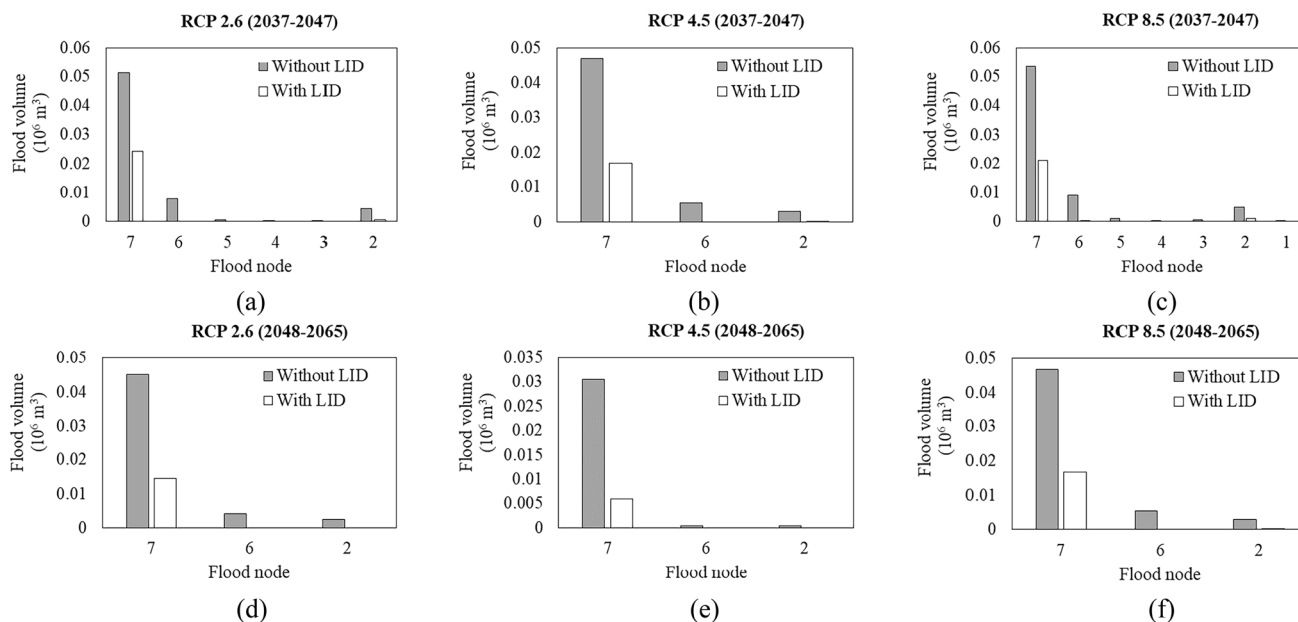


Fig. 7 Comparison of flood volume with and without LID under the near future for **a** RCP 2.6, **b** RCP 4.5, **c** RCP 8.5; and under the far future for **d** RCP 2.6, **e** RCP 4.5, and **f** RCP 8.5

There is no specific pattern for rainfall reduction with respect to the emission scenarios. Stormwater was simulated in the study area with the SWMM with and without the LID SCMs. The flood volume at each node (nodes 1 to 7) in the study area and the maximum runoff volume at the basin outlet were calculated for the baseline period with the design rainfall as input to the SWMM under emission scenarios RCP 2.6, RCP 4.5, and RCP 8.5 in the near and far future.

The results indicate that the use of LID SCMs in the context of climate change would reduce the volume of runoff. The LID SCMs would reduce the flood volume in the near future by 22%, 23%, and 21% under the RCP2.6, RCP4.5, and RCP8.5, respectively, and they would reduce the flood volume in the far future by 23%, 27%, and 23% under the RCP2.6, RCP4.5, and RCP8.5 scenarios, respectively. Therefore, the largest reduction in flood volume in the near future corresponds to the RCP4.5 scenario with about 23% and in the far future in the same scenario with about 27%. The deployment of LID SCMs would reduce the number of floods by 50%, which constitutes a significant improvement of the drainage system in the study region basin. Future research will apply evolutionary algorithms to minimize stormwater with LID SCMs.

Author contribution Manizheh Pournali Dougaheh developed the theory and performed the computations. Parisa-Sadat Ashofteh encouraged Manizheh Pournali Dougaheh to investigate a specific aspect. Parisa-Sadat Ashofteh supervised the findings of this work, and Hugo A. Loáiciga helped supervise the project. All authors discussed the results and

contributed to the final manuscript. Manizheh Pournali Dougaheh wrote the manuscript with support from Parisa-Sadat Ashofteh and especially Hugo A. Loáiciga. Parisa-Sadat Ashofteh conceived the original idea.

Data availability Data will be made available on reasonable request.

Code availability Code will be made available upon reasonable request.

Declarations

Ethics approval All procedures performed in studies are in accordance with the ethical standards.

Consent to participate The authors voluntarily agreed to participate in this research study.

Consent for publication The authors agree to the publication of this paper.

Conflict of interest The authors declare no competing interests.

References

- Aminjavaheri SM, Nazif S (2018) Determining the robust optimal set of BMPs for urban runoff management in data-poor catchments. *J Environ Plan Manag* 6:1180–1203
- Ashofteh P-S, Bozorg-Haddad O, Mariño M (2013a) Climate change impact of on reservoir performance indexes in agricultural water supply. *J Irrig Drain Eng* 139(2):85–97. [https://doi.org/10.1061/\(ASCE\)IR.1943-4774.0000496](https://doi.org/10.1061/(ASCE)IR.1943-4774.0000496)
- Ashofteh P-S, Bozorg-Haddad O, Mariño MA (2013b) Scenario assessment of streamflow simulation and its transition probability in future periods under climate change. *Water Resour Manag* 27(1):255–274. <https://doi.org/10.1007/s11269-012-0182-2>

- Bahrami M, Bozorg-Haddad O, Loáiciga HA (2019) Optimizing stormwater low-impact development strategies in an urban watershed considering sensitivity and uncertainty. *Environ Monit Assess* 191(6):1–14. <https://doi.org/10.1007/s10661-019-7488-y>
- Bai Y, Zhao N, Zhang R, Zeng X (2019) Storm water management of low impact development in urban areas based on SWMM. *Water* 11(1):33. <https://doi.org/10.3390/w11010033>
- Bell FC (1969) Generalized rainfall-duration-frequency relationship. *J Hydraul Div* 95(1):311–327
- Chang N-B, Lu J-W, Chui TFM, Hartshorn N (2018) Global policy analysis of low impact development for stormwater management in urban regions. *Land Use Policy* 70:368–383
- Chow VT, Maidment DR, Mays LW (1988) *Applied Hydrology*. McGraw Hill, New York, York, NY, USA, p 572
- Eckart K, McPhee Z, Bolisetti T (2018) Multiobjective optimization of low impact development stormwater controls. *J Hydrol* 562:564–576
- Gao C, Hao M, Chen J, Gu C (2021) Simulation and design of joint distribution of rainfall and tide level in Wuchengxiyu Region, China. *Urban Clim* 40:101005. <https://doi.org/10.1016/j.uclim.2021.101005>
- Gahreman B (1996) Updated IDF equation for rainfall in Iran using 1-hour, 10-year rainfall. *J Agric Sci* 6:13–30 (in Persian)
- Gogate NG, Kalbar PP, Raval PM (2017) Assessment of stormwater management options in urban contexts using multiple attribute decision-making. *J Clean Prod* 142:2046–2059
- Helmi NR, Verbeiren B, Mijic A, van Griensven A, Bauwens W (2019) Developing a modeling tool to allocate low impact development practices in a cost-optimized method. *J Hydrol* 573:98–108
- Hua P, Yang W, Qi X, Jiang S, Xie J, Gu X, Li H, Zhang J, Krebs P (2020) Evaluating the effect of urban flooding reduction strategies in response to design rainfall and low impact development. *J Clean Prod* 242:118515. <https://doi.org/10.1016/j.jclepro.2019.118515>
- IPCC. (2001). *Climate change 2001: synthesis report. A Contribution of Working Groups I, II, and III to the Third Assessment Report of the Intergovernmental Panel on Climate Change* [Watson, R.T. and the Core Writing Team (eds.)]. Cambridge University Press, Cambridge, United Kingdom, and New York, NY, USA, pp. 398
- Jones PD, Hulme M (1996) Calculating regional climate times series for temperature precipitation: methods and illustrations. *Int J Climatol* 16:361–377
- Liu Y, Zhang K, Li Z, Liu Z, Wang J, Huang P (2020) A hybrid runoff generation modeling framework based on spatial combination of three runoff generation schemes for semi-humid and semi-arid watersheds. *J Hydrol* 590:125440. <https://doi.org/10.1016/j.jhydrol.2020.125440>
- Loáiciga HA, Sadeghi KM, Shivers S, Kharaghani S (2015) Stormwater control measures: optimization methods for sizing and selection. *J Water Resour Plan Manag* 141:04015006. [https://doi.org/10.1061/\(ASCE\)WR.1943-5452.0000503](https://doi.org/10.1061/(ASCE)WR.1943-5452.0000503)
- Mahab Ghodss Consulting Engineering Company (2012) *Comprehensive plan of Tehran surface water management*, vol 11. Mahab Ghodss Consulting Engineering Company, pp 241–232
- Mani M, Bozorg-Haddad O, Loáiciga HA (2019) A new framework for the optimal management of urban runoff with low-impact development stormwater control measures considering service-performance reduction. *J Hydroinf* 21(5):727–744
- Oliazadeh A, Bozorg-Haddad O, Mani M, Chu X (2021) Developing an urban runoff management model by using satellite precipitation datasets to allocate low impact development systems under climate change conditions. *Theor Appl Climatol* 146:675–687
- Pour SH, Abd Wahab AK, Shahid S, Asaduzzaman M, Dewan A (2020) Low impact development techniques to mitigate the impacts of climate-change-induced urban floods: current trends, issues and challenges. *Sustain Cities Soc* 62:102373. <https://doi.org/10.1016/j.scs.2020.102373>
- Quan Q, Liang W, Yan D, Lei J (2022) Influences of joint action of natural and social factors on atmospheric process of hydrological cycle in Inner Mongolia, China. *Urban Clim* 41:101043. <https://doi.org/10.1016/j.uclim.2021.101043>
- Saadatpour M, Delkhosh F, Afshar A, Solis SS (2020) Developing a simulation-optimization approach to allocate low impact development practices for managing hydrological alterations in urban watershed. *Sustain Cities Soc* 61:102334. <https://doi.org/10.1016/j.scs.2020.102334>
- Sadeghi KM, Loáiciga HA, Kharaghani S (2018) Stormwater control measures for runoff and water quality management in urban landscapes. *J Am Water Resour Assoc* 54:1–10. <https://doi.org/10.1111/1752-1688.12547>
- Wang M, Zhang D, Cheng Y, Tan SK (2019) Assessing performance of porous pavements and bioretention cells for stormwater management in response to probable climatic changes. *J Environ Manag* 243:157–167
- Wang M, Zhang DQ, Su J, Dong JW, Tan SK (2018) Assessing hydrological effects and performance of low impact development practices based on future scenarios modeling. *J Clean Prod* 179:12–23
- Xiao M, Li Y, Huang JJ (2021) Optimization of low impact development based on SWMM and genetic algorithm: case study in Tianjin, China. In: *EGU General Assembly Conference Abstracts*, p 8154
- Zahmatkesh Z, Burian SJ, Karamouz M, Tavakol-Davani H, Goharian E (2015) Low-impact development practices to mitigate climate change effects on urban stormwater runoff: Case study of New York City. *J Irrig Drain Eng* 141(1):04014043
- Zhang P, Ariaratnam ST (2020) Life cycle cost savings analysis on traditional drainage systems from low impact development strategies. *Front Eng Manag* 8:1–10

Publisher's note Springer Nature remains neutral with regard to jurisdictional claims in published maps and institutional affiliations.

Springer Nature or its licensor (e.g. a society or other partner) holds exclusive rights to this article under a publishing agreement with the author(s) or other rightsholder(s); author self-archiving of the accepted manuscript version of this article is solely governed by the terms of such publishing agreement and applicable law.